http://dx.doi.org/10.5012/bkcs.2014.35.10.2917

Template-free Synthesis and Characterization of Spherical $Y_3Al_5O_{12}:Ce^{3+}$ (YAG:Ce) Nanoparticles

Taekeun Kim and Jin-Kyu Lee*

*Department of Chemistry, Seoul National University, Seoul 151-747, Korea. *E-mail: jinklee@snu.ac.kr*
Received June 2, 2014, Accepted June 5, 2014

Cerium-activated yttrium aluminate ($Y_3Al_5O_{12}:Ce^{3+}$) exhibiting a garnet structure has been widely utilized in the production of light emitting diodes (LEDs) as a yellow emitting phosphor. The commercialized yttrium aluminum garnet (YAG) phosphor is typically synthesized by a solid-state reaction, which produces irregular shape particles with a size of several tens of micrometers by using the top-down method. To control the shape and size of particles, which had been the primary disadvantage of top-down synthetic methods, we synthesized YAG:Ce nanoparticles with a diameter of 500 nm using a coprecipitation method under the atmospheric pressure without the use of template or special equipment. The precursor particles were formed by refluxing an aqueous solution of the nitrate salts of Y, Al, and Ce, urea, and polyvinylpyrrolidone (55 K) at 100 °C for 12 h. YAG:Ce nanoparticles were formed by the calcination of precursor particles at 1100 °C for 10 h under atmospheric conditions. The phase identification, microstructure, and photoluminescent properties of the products were evaluated by X-ray powder diffraction, scanning electron microscopy, absorption spectrum and photoluminescence analyses.

Key Words : Yttrium aluminum garnet, Cerium doping, Phosphor nanoparticle, Template-free synthesis, Co-precipitation

Introduction

Solid-state lighting systems based on light emitting diodes (LEDs) consume very little power and do not contain any of the harmful heavy metals that are often found in conventional incandescent light bulbs and fluorescent lamps. Therefore, solid-state lighting systems have been widely utilized as a light source, especially for the back-light units of portable display devices.[1-4] Currently, the simplest and most widely used white LED system employs blue light emitting GaN as the light source and a cerium-doped yttrium aluminum garnet ($Y_3Al_5O_{12}:Ce^{3+}$) phosphor as the color converter.[5,6] Although commercialized white LEDs containing YAG phosphors that are several tens of micrometers produce desirable stabilities and photoluminescent efficiencies,[7] there are still drawbacks associated with the large size and non-uniform shape of the YAG phosphor such as inhomogeneous mixing which subsequently results in the relatively low reproducibility of the quality of white LEDs.

To address these challenges, investigations into the production of nano-sized YAG phosphors have been currently executed.[8-11] There are two primary approaches to the synthesis of nano-sized YAG phosphors. The first approach is a top-down method where bulk YAG synthesized by the conventional solid-state diffusion reaction technique is pulverized into nano-sized particles using ball-mill equipment. This method is not effective in forming nano-sized YAG phosphors with a narrow size distribution, regular shape, and homogeneity. Furthermore, the photoluminescence (PL) efficiency is often significantly reduced because of defects generated during the ball-mill process.[12] The second approach to synthesizing nano-sized YAG particles is the bottom-up method, which is a wet-chemical method that utilizes reactions in solution. Since solution-based syntheses can yield better homogeneity,[13-15] there have been several investigations regarding the wet-chemical synthesis of nano-sized YAG phosphors that employed sol-gel,[13,16-18] co-precipitation,[19-21] homogeneous precipitation,[22] spray pyrolysis,[23,24] hydrothermal reaction,[25] and combustion methods.[14] Although several researchers have previously produced nano-sized YAG phosphors by the simple co-precipitation method, their syntheses often required special equipment such as an autoclave to form the nanoparticles at high temperatures and pressures.[26,27] Whenever YAG phosphors were produced at room temperature under atmospheric pressure without the use of templates, they often formed large particles with a diameter of several micrometers with a broad size distribution.[28,29]

In this study, we synthesized Ce^{3+}-doped spherical nano-sized YAG phosphors by the co-precipitation method using a nitrate source as the starting material in an aqueous solution without the use of special equipment or templates. Urea was used as the base and poly(vinylpyrrolidone) (PVP) was added as a mediator to form spherical precursor nanoparticles. After calcination of precursor particles at 1100 °C for 10 h under atmospheric conditions, YAG:Ce phosphors with a diameter of 500 nm and exhibiting a multi-granular spherical shape were successfully synthesized and their properties were subsequently investigated.

Experimental

Chemicals and Instrumentation. Aluminum nitrate, yttrium

nitrate, cerium nitrate and poly(vinylpyrrolidone) (55 K) were purchased from Aldrich. Urea, ethanol, and acetone were purchased from Samchun Chemical. All chemicals were used without further purification. UV-Vis and PL spectra were recorded on a Scinco S-3100 and Jasco FP-6500 spectrophotometer, respectively. X-ray powder diffraction (XRD) measurements were carried out on D8 Advance (Bruker) and M18XHF-SRA (MAC Science Co.) instruments. Field-emission scanning electron microscope (FE-SEM) and cathode luminescence (CL) experiments were carried out using Hitachi-S4300 (Hitachi) and Gatan-MonoCL4 instruments, respectively.

Synthesis of Precursor Particles. $Al(NO_3)_3$, $Y(NO_3)_3$, and $Ce(NO_3)_3$ were mixed in 100 mL of water at the ratio of Y:Al:Ce = (0.6–x):1:x (mmol). The amount of $Ce(NO_3)_3$ was varied between approximately 0.03-0.04 mmol. An excess of urea (0.2 g) and PVP (4 g) were added to the mixed solution, which was then refluxed for 12 h. The YAG:Ce precursor particles were generated by the reaction of the nitrate sources with hydroxide and carbonate ions as the urea slowly decomposed at temperature above 90 °C.[30]

To remove the excess PVP and other side products, acetone was added to the solution containing the YAG:Ce precursor particles in a 1:1 ratio, and the solution was then centrifuged at 7000 rpm to isolate the products. This purification process was repeated two more times by being redispersed in ethanol and centrifuged at 7000 rpm to yield YAG:Ce particles with a diameter of approximately 1 mm.

Calcination Process to Synthesize the YAG:Ce Nanoparticles. The synthesized precursor particles were dried in a vacuum oven at 90 °C for 6 h, and the YAG:Ce nanoparticles were then synthesized upon calcination at 1100 °C (with a heating rate of 4 °C/min) for 10 h.

Results and Discussion

The morphology and structure of the synthesized precursor particles were analyzed by FE-SEM. Figure 1 displays the particles formed by the reaction of the nitrate sources with urea in the presence of PVP (55 K) at 100 °C for 12 h. The ratio of Ce^{3+} was varied between 0.03 and 0.05 mmol (where Y:Al:Ce = (0.6–x):1:x). The spherical particles exhibited a diameter of approximately 1 μm in the shape of dandelion seeds, regardless of the Ce doping ratio.

Figure 2 shows the morphology of the precipitates measured by FE-SEM, which were separated from an aliquot taken during the formation of precursor particles. As urea decomposes at 100 °C, it reacts with $Al(NO_3)_3$, $Y(NO_3)_3$ and $Ce(NO_3)_3$ to induce precipitation of the hydroxycarbonate forms, having the assumed formula of $Y_{(3-x)}Al_5Ce_x(OH)_{16}(CO_3)_4{\cdot}4H_2O$ based on the previous investigations.[30] These mixed precipitates were then aggregated in the presence of PVP (which acts as a mediator in solution) and the aggregates then formed the 500 nm bar shapes as shown in Figure 2(a). This unit particle was continuously assembled as the reaction proceeded (Figure 2(b)) and spherical particles with a diameter of approximately 1 μm size were finally produced (Figure 2(c)).

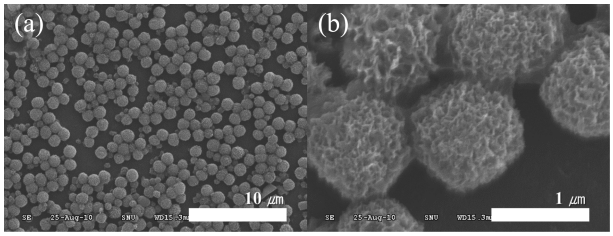

Figure 1. FE-SEM images of template-free precursor particles at different magnifications; the scale bar shown in (a) is 10 μm and in (b) is 1 μm.

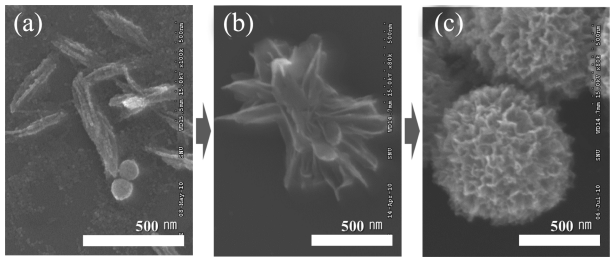

Figure 2. FE-SEM images obtained during the formation of the precursor particles; after (a) 2, (b) 6, and (c) 12 h at 100 °C.

The precursor particles, which appeared in the shape of dandelion seeds at 100 °C after 12 h, were isolated and redispersed in ethylene glycol (which has higher boiling point) and the solution was heated at 150 °C for 12-36 h. As a result, the diameter of the precursor particles increased to 1.5-2 μm, as shown in Figure 3. It appeared that the particle size increased as a result of the ripening process when the precursor particles were heated in ethylene glycol. The size of the precursor particles increased as the heating temperature increased as a result of the temperature-dependent assembly processes. Some particles appeared to be cross-sectioned, as shown in Figure 3(d). The unit particles that were 500 nm in length (Figure 2(a)) were rearranged like the

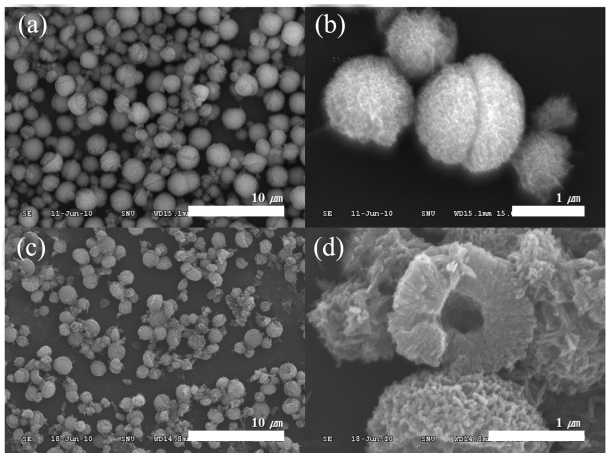

Figure 3. FE-SEM images of the precursor particles after post-treatment at 150 °C in ethylene glycol; (a) and (b) after 12 h, and (c) and (d) after 36 h.

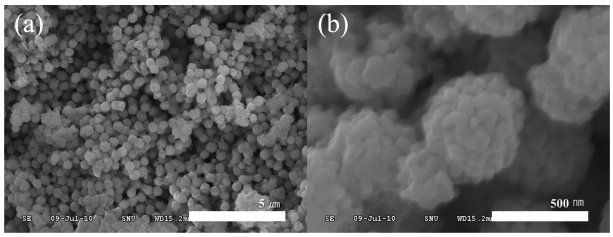

Figure 4. FE-SEM images of the YAG:Ce nanoparticles synthesized through calcination at 1100 °C for 10 h.

spokes of a wheel at higher temperatures. As a result, a particle with a diameter of approximately 1.5-2 μm was formed by the unit particles. Therefore, a hollow structure was formed.

The spherical precursor particles, which formed in the shape of dandelion seeds at 100 °C after 12 h heating in an aqueous solution, were dried in a vacuum oven at 90 °C which resulted in a reduction of the diameter to 700 nm (data not shown). This result was attributed to the evaporation of solvent within the sparse and wrinkled structure of precursor particles during the drying process.

YAG:Ce nanoparticles with a diameter of approximately 500 nm were prepared by the calcination of the precursor particles using a furnace under atmospheric pressure at 1100 °C for 10 h and exhibited a multi-granular structure with diameters of 50-100 nm, as shown in Figure 4. The crystal structure of the synthesized nanoparticles was confirmed by using XRD. Figure 5 displays the XRD pattern of the YAG:Ce nanoparticles when the Ce^{3+} doping level was 1% (Y:Al:Ce = 2.97:5:0.03) of Y^{3+}, which closely matched the known patterns of the YAG phase (JCPDS No. 33-0040). It was also verified that the YAG:Ce nanoparticles exhibited desirable crystallinity after the calcination process at 1100 °C for 10 h and did not contain a phase corresponding to CeO_2 (JCPDS No. 34-0394) as a result of the very low doping level of Ce^{3+} in YAG. It has been previously reported that the fluorescence of YAG:Ce would decrease if the doping concentration of Cd^{3+} is high enough to observe the XRD phase of CeO_2. According to the results of the experiments containing various doping concentrations of Ce^{3+}, we verified that the highest fluorescence was obtained when the concentration of Ce^{3+} was 1.0-1.4% relative to Y^{3+} (data not shown), which was consistent with the results in the literature.[27,31]

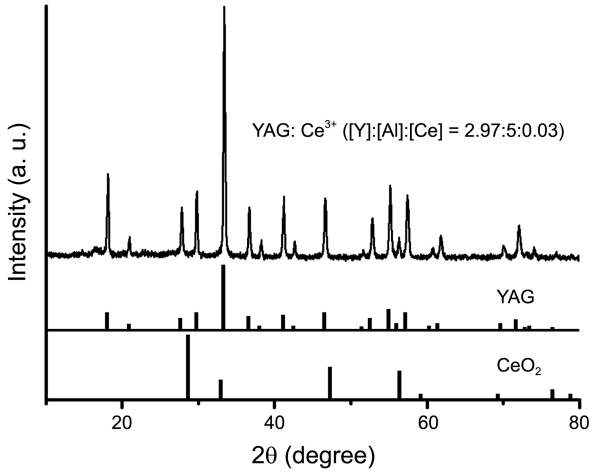

Figure 5. XRD pattern of the prepared YAG:Ce nanoparticles.

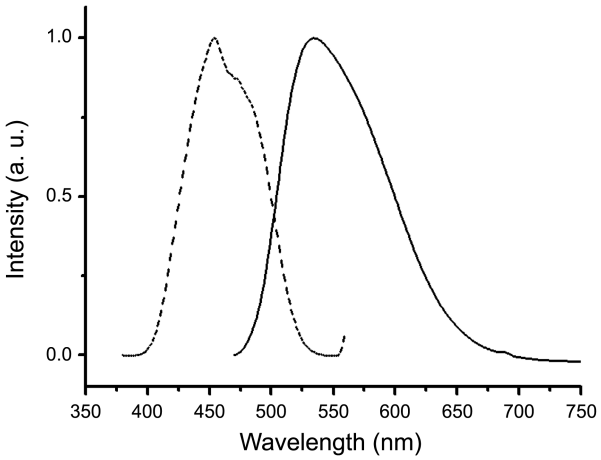

Figure 6. Excitation (dashed line) and PL (solid line) spectra of the YAG:Ce^{3+} nanoparticle powder.

YAG:Ce nanoparticles with a Ce^{3+} doping level of 1.0% produce yellow luminescence in the powder form, as shown in Figure 6. The maximum of the excitation peak was observed at 450 nm with respect to the PL excitation spectrum (λ_{em} = 570 nm), while the emission exhibited a 534 nm peak and shoulder in the longer wavelength region (λ_{ex} = 460 nm). This emission is a characteristic of Ce^{3+} ions within the garnet crystalline lattice (cubic-$Y_3Al_5O_{12}$), corresponding to the $5d(^2A_{1g}) \rightarrow 4f(^2F_{7/2})$ transition.[26,28,32]

YAG:Ce nanoparticles synthesized in this study exhibited a PL intensity of approximately 20% compared to the commercialized phosphor, despite exhibiting a desirable crystallinity. To determine why the synthesized YAG:Ce nanoparticles exhibited a lower PL emission than the phosphor synthesized by solid-state reaction, we verified whether each YAG:Ce nanoparticle exhibited a uniform PL emission by evaluating the cathode luminescence (CL) images. Figure 7 shows a sample calcined at 1100 °C for 10 h after the precursor particles were mixed with 350 nm silica nanoparticles as a solid diluent to prevent the direct aggregation of

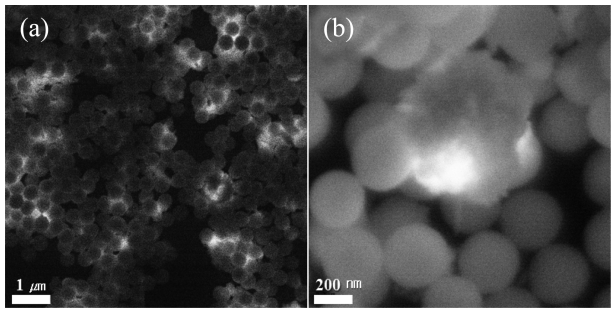

Figure 7. CL images of the YAG:Ce nanoparticles mixed with 350 nm silica nanoparticles at different magnifications; the scale bar shown in (a) is 1 μm, and in (b) is 200 nm.

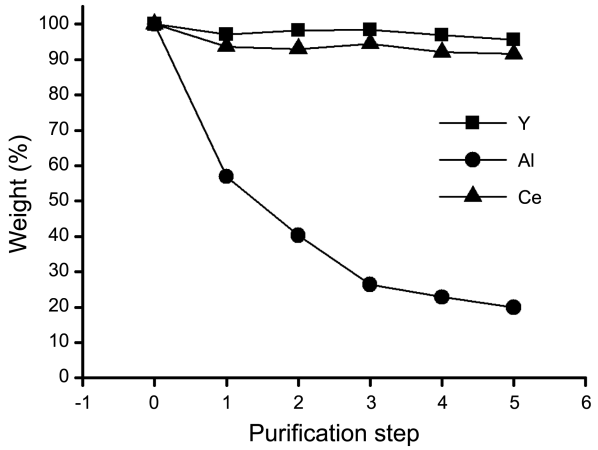

Figure 8. The weight loss profiles of each hydroxycarbonate precipitate during the purification process with ethanol.

YAG:Ce particles as well as any unexpected crystal growth. In the CL images of Figure 7, it was clearly observed that the YAG:Ce nanoparticles within the fused silica nanoparticles emitted light. However, in Figure 7(b), it was clearly observed that the entire area of one YAG:Ce nanoparticle that was located on the surface does not emit uniformly and only portion of particle exhibited bright emission, which was likely a result of the inhomogeneous composition of the synthesized YAG:Ce crystal.

To determine the cause of the formation of the inhomogeneous YAG:Ce nanoparticles, we evaluated the relative solubility of the hydroxycarbonate precipitates generated by the reaction of the nitrates of each metal with urea under the same conditions that formed the YAG:Ce precursor particles, using 1.28 mmol of each starting material. Each precipitated Y, Al, and Ce hydroxycarbonate was completely dried in the vacuum oven and washed with ethanol to rinse the mixed hydroxycarbonate precipitates and remove any excess PVP and other side products. In each ethanol washing step, the amount of weight loss was precisely measured using an analytical balance. As shown in Figure 8, aluminum hydroxycarbonate was almost completely removed during the washing steps with ethanol, while the amount of yttrium hydroxycarbonate and cerium hydroxycarbonate remained nearly constant. The ratio of yttrium, aluminum, and cerium ions is the most important factor in the synthesis of the high quality YAG:Ce phosphors. It has been previously reported that the fluorescence intensity may decrease or the garnet crystalline lattice (cubic-$Y_3Al_5O_{12}$) may not form, if the YAG:Ce nanoparticles are synthesized under conditions where the ratio was not properly maintained.[27,31] Therefore, YAG:Ce nanoparticles prepared through our synthetic methodology exhibited a relatively low PL efficiency due to the inhomogeneity of chemical composition, and further investigations are currently under way to address this issue.

Conclusion

Spherical YAG:Ce nanoparticles were successfully prepared by a simple co-precipitation method without employing any special equipment or templates. We analyzed the morphology and structure of the materials during the formation of the precursor particle, and synthesized YAG:Ce nanoparticles with a diameter of approximately 500 nm upon calcination at 1100 °C. The crystal structure of the synthesized YAG:Ce nanoparticles was characterized using XRD to verify the Ce^{3+}-doped garnet crystalline lattice (cubic-$Y_3Al_5O_{12}$) structure, and the optical properties were evaluated using PL excitation and emission spectra. We also investigated the cause for the formation of inhomogeneous YAG:Ce nanoparticles by comparing the relative solubilities of hydroxycarbonate precipitates during the purification process. We believe that the method described in this report is an alternate approach to synthesize YAG:Ce nanoparticles in a manner that is both simple and easily scalable. Additionally, we determined that the relative solubility of the starting materials has a direct impact on the homogeneity of the produced YAG:Ce nanoparticles, and can provide key insights in the preparation of the high quality YAG:Ce nanoparticle phosphors.

Acknowledgments. This work was partially supported by the Nano R&D Program (2012-0006209) through the National Research Foundation of Korea (NRF) funded by the Ministry of Education, Science, and Technology of Korea; and an industrial fund from Samsung Electronics Co., Ltd. T. Kim is grateful for the award of the BK21 fellowship.

References

1. Moreno, I.; Sun, C. C. *Opt. Express* **2008**, *16*, 1808.
2. Pereira, P. F. S.; Matos, M. G.; Avila, L. R.; Nassor, E. C. O.; Cestari, A.; Ciuffi, K. J.; Calefi, P. S.; Nassar, E. J. *J. Lumin.* **2010**, *130*, 488.
3. Bhat, S. V.; Govindaraj, A.; Rao, C. N. R. *Chem. Phys. Lett.* **2006**, *422*, 323.
4. Shao, Q. Y.; Li, H. J.; Dong, Y.; Jiang, J. Q.; Liang, C.; He, J. H. *J. Alloy. Compd.* **2010**, *498*, 199.
5. Xia, G. D.; Zhou, S. M.; Zhang, J. J.; Xu, J. *J. Cryst. Growth* **2005**, *279*, 357.
6. Kim, H. T.; Kim, J. H.; Hong, Y. J.; Lee, J. K.; Kang, Y. C. *Electron. Mater. Lett.* **2012**, *8*, 283.
7. Mueller-Mach, R.; Mueller, G. O.; Krames, M. R.; Trottier, T. *Ieee J. Sel. Top. Quant.* **2002**, *8*, 339.
8. Huczko, A.; Kurcz, M.; Baranowski, P.; Bystrzejewski, M.; Bhattarai, A.; Dyjak, S.; Bhatta, R.; Pokhrel, B.; Kafle, B. P. *Phys. Status Solidi B* **2013**, *250*, 2702.
9. Chen, Z. H.; Yang, Y.; Hu, Z. G.; Li, J. T.; He, S. L. *J. Alloy. Compd.* **2007**, *433*, 328.
10. Hassanzadeh-Tabrizi, S. A. *Adv. Powder Technol.* **2012**, *23*, 324.
11. Li, X. X.; Zheng, B. Y.; Odoom-Wubah, T.; Huang, J. L. *Ceram. Int.* **2013**, *39*, 7983.
12. Song, H. J.; Noh, J. H.; Roh, H. S.; Kim, J. S.; Kim, D. W.; Hong, K. S. *Curr. Appl. Phys.* **2013**, *13*, S69.
13. Popovici, E. J.; Morar, M.; Bica, E.; Perhaita, I.; Cadis, A. I.; Indrea, E.; Barbu-Tudoran, L. *J. Optoelectron. Adv. M* **2011**, *13*, 617.
14. Popovici, E. J.; Muresan, L.; Amalia, H.; Indrea, E.; Vasilescu, M. *J. Alloy. Compd.* **2007**, *434*, 809.
15. Muresan, L.; Popovici, E. J.; Grecu, R.; Tudoran, L. B. *J. Alloy. Compd.* **2009**, *471*, 421.

16. Kottaisamy, M.; Thiyagarajan, P.; Mishra, J.; Rao, M. S. R. *Mater. Res. Bull.* **2008**, *43*, 1657.
17. Ye, S.; Xiao, F.; Pan, Y. X.; Ma, Y. Y.; Zhang, Q. Y. *Mat. Sci. Eng. R* **2010**, *71*, 1.
18. Won, C. W.; Nersisyan, H. H.; Won, H. I.; Lee, J. H.; Lee, K. H. *J. Alloy. Compd.* **2011**, *509*, 2621.
19. Murai, S.; Fujita, K.; Iwata, K.; Tanaka, K. *Opt. Mater.* **2010**, *33*, 123.
20. Yang, Z. P.; Li, X.; Yang, Y.; Li, X. M. *J. Lumin.* **2007**, *122*, 707.
21. Jia, N. T.; Zhang, X. D.; He, W.; Hu, W. J.; Meng, X. P.; Du, Y.; Jiang, J. C.; Du, Y. W. *J. Alloy. Compd.* **2011**, *509*, 1848.
22. Lee, S. H.; Jung, D. S.; Han, J. M.; Koo, H. Y.; Kang, Y. C. *J. Alloy. Compd.* **2009**, *477*, 776.
23. Wang, Y.; Yuan, P.; Xu, H. Y.; Wang, J. Q. *J. Rare Earth.* **2006**, *24*, 183.
24. Chiang, C. C.; Tsai, M. S.; Hsiao, C. S.; Hon, M. H. *J. Alloy. Compd.* **2006**, *416*, 265.
25. Ogata, H.; Takeshita, S.; Isobe, T.; Sawayama, T.; Niikura, S. *Opt. Mater.* **2011**, *33*, 1820.
26. Kasuya, R.; Isobe, T.; Kuma, H.; Katano, J. *J. Phys. Chem. B* **2005**, *109*, 22126.
27. Yang, H. J.; Yuan, L.; Zhu, G. S.; Yu, A. B.; Xu, H. R. *Mater. Lett.* **2009**, *63*, 2271.
28. Marius, M.; Popovici, E. J.; Barbu-Tudoran, L.; Indrea, E.; Mesaros, A. *Ceram. Int.* **2014**, *40*, 6233.
29. Yang, S. K.; Que, W. X.; Chen, J.; Liu, W. G. *Ceram. Int.* **2012**, *38*, 3185.
30. Sordelet, D. J.; Akinc, M.; Panchula, M. L.; Han, Y.; Han, M. H. *J. Eur. Ceram. Soc.* **1994**, *14*, 123.
31. Purwanto, A.; Wang, W. N.; Ogi, T.; Lenggoro, I. W.; Tanabe, E.; Okuyama, K. *J. Alloy. Compd.* **2008**, *463*, 350.
32. Lu, C. H.; Hong, H. C.; Jagannathan, R. *J. Mater. Chem.* **2002**, *12*, 2525.